

PROCEEDINGS OF SPIE

SPIDigitalLibrary.org/conference-proceedings-of-spie

Plane wave acousto-optic imaging in reflection mode geometry

Nowak, Lukasz, Steenbergen, Wiendelt

Lukasz J. Nowak, Wiendelt Steenbergen, "Plane wave acousto-optic imaging in reflection mode geometry," Proc. SPIE 11642, Photons Plus Ultrasound: Imaging and Sensing 2021, 116424R (5 March 2021); doi: 10.1117/12.2576348

SPIE.

Event: SPIE BiOS, 2021, Online Only

Plane wave acousto-optic imaging in reflection mode geometry

Lukasz J. Nowak^a and Wiendelt Steenbergen^a

^aBiomedical Photonic Imaging Group, Faculty of Science and Technology, University of Twente, P.O. Box 217, 7500 AE, Enschede, The Netherlands

ABSTRACT

Imaging performance of an acousto-optic system is limited by light fluence rate and acoustic pressure field distributions characteristics. The system parameters can be shaped by changing relative positions of ultrasound transducer array and optodes. However, in case of many potential clinical applications optimization possibilities in this regard are limited, as a sample is accessible from one side only and using a water tank for coupling is not feasible. We investigate the possibilities of improving performance of an acousto-optic imaging system operating in reflection mode geometry with linear ultrasound array in direct contact with a sample by using plane wave instead of focused ultrasound pulses. Differences in acoustic pressure field distributions for various transducer excitation patterns were determined numerically. Acousto-optic images of phantoms with and without optically absorbing inclusions were acquired by measuring laser speckle contrast decrease due to the light modulation by plane wave and focused ultrasound pulses. The light fluence rate maps reconstructed using plane wave imaging proved more distinct and clear.

Keywords: acousto-optic imaging; plane wave; reflection mode; ultrasound linear array

1. INTRODUCTION

We investigate the possibilities of improvements of imaging performance of a reflection-mode acousto optic imaging (AOI) system with linear ultrasound (US) array by using plane-wave acoustic pulses instead of focused ones. In principle, AOI allows to determine fluence rate distribution of light transmitted through an optically-scattering medium by exploiting effects of interaction between the light and an acoustic wave. Due to the induced motion of optical scatterers within the illuminated and insonified volume, the light that is scattered within this region undergoes modulation (the acousto-optic effect)^{1,2}. By determining the ratio of intensities of modulated to non-modulated light for various acoustic pressure field distributions, the fluence rate map in the medium can be determined. This in turn can be - under certain conditions - used to detect and localize optically absorbing inclusions inside the region of interest.³

Comprehensive reviews of various studies on AOI were presented by Elson et al.,⁴ Resink et al.,⁵ and Gunther and Andersson-Engels.⁶ The presented solutions differ in various aspects, including configuration of optodes, US transducer type and position relative to sample, signal detection means, and combination with other imaging modalities. In the present study we consider a reflection mode AOI, i.e. configuration in which both optodes and US transducer are positioned on the same side of an investigated sample. Such a configuration was previously investigated by Lev et al.,⁷⁻⁹ Hisaka and Saskura,¹⁰ Kim et al.,¹¹ and Hong-Bo et al.¹² In all of these investigations the imaging was performed by physically changing the relative positions of the investigated sample and the probe, while keeping the US focus constant. As we have demonstrated in our previous study,³ such an approach allows to directly link the observed changes of the received signal with changes of optical properties within the region of interest. Here, we impose a condition that the measurement probe should remain stationary relative to the sample during the whole imaging procedure. The introduced restrictions are in accordance with practical limitations related to various clinical problems, in which the region of interest is accessible from one side only, and physical scanning might be not feasible or not desired.

Further author information:

Lukasz J. Nowak: E-mail: l.j.nowak@utwente.nl, Telephone: +31534891974

Photons Plus Ultrasound: Imaging and Sensing 2021, edited by Alexander A. Oraevsky
Lihong V. Wang, Proc. of SPIE Vol. 11642, 116424R · © 2021 SPIE
CCC code: 1605-7422/21/\$21 · doi: 10.1117/12.2576348

Proc. of SPIE Vol. 11642 116424R-1

The detected acousto-optic signal is proportional to the product of light fluence rate and acoustic pressure amplitude squared, integrated over the whole volume of interest.^{2,13} In the considered case of static probe and sample, the fluence rate distribution remains constant, while the acoustic pressure field distribution is subject to change in order to perform scanning and image reconstruction. Typically, focused US pulses are used for light modulation in order to maximize the achievable acoustic pressure amplitude and minimize the insonified volume. It is then assumed that the acoustic pressure field distribution is entirely concentrated within the desired focal region, and by scanning the US focus and measuring AOI signal, the light fluence rate map is reconstructed.³ The accurateness of such an assumption, however, strongly depends on transducer type and excitation scheme. In general, focusing of US pulses is achieved either by using specially shaped electroacoustic transducers with constant focus, and/or by using a matrix of singly driven transducer elements with excitation delays determined in such a way that constructive interference between all the emitted pulses occurs at the desired focal point. Based on the fundamental principles of operation of any US transducer matrix, one can expect that some residual pressure field components will also be present in the surrounding space – although their amplitudes should be significantly lower than in the focal region.¹⁴ On the other hand, they may also occupy much greater volume and in this way have significant influence on the determined acousto-optic signal.

Using plane wave US pulses for AOI was previously investigated by Lauderan et al.¹⁵ and by Bocoum et al.^{16,17} The authors also used linear transducer array, but their setups were arranged in transmission-mode geometry. The studies focused on using plane-wave pulses emitted at multiple angles and applying novel image reconstruction algorithms for improved image quality and data acquisition time. The authors did not consider the influence of residual acoustic pressure field components, despite noting that uncontrolled diffraction effects may limit the system performance when applying additional US wavefront shaping.¹⁶

The aim of the present study is to investigate the influence of the residual acoustic pressure field components (i.e. the non-zero pressure field components outside the desired imaging region) and mitigate their influence on the resulting acousto-optic image in the given reflection-mode configuration with the probe in direct contact with a sample.

2. MATERIALS AND METHODS

The first part of the present study were numerical simulations of acoustic pressure field distributions obtained using a 1-D US transducer array and various excitation schemes. The results of these computations were used to explain the outcomes of experimental investigations on reflection mode AOI, conducted using analogous US pulse patterns. The details regarding the adopted approaches are presented below.

2.1 Numerical simulations

Numerical simulations of acoustic pressure field distributions were conducted using k-Wave simulation package for Matlab, and Matlab scripts for data post-processing, analysis and visualization. We used a 3-D cuboid mesh with dimensions 49 mm (axial) x 49 mm (lateral) x 23,3 mm (elevation), divided into 488 x 488 x 232 grid elements. Additional 12 grid elements at each side constituted perfectly matched layer to simulate free-field conditions.

The simulated US linear array consisted of 128 rectangular transducer elements with dimensions 301 μm (width, lateral; 3 grid points) x 4 mm (length, elevation; 40 grid points). The elements were positioned directly next to each other. A constant focus in the elevation direction was set to 25 mm by applying variable excitation delays to the source grid points along the lengths of the elements, using one of the built-in k-Wave functions. All the parameters were chosen in such a way, to approximate the geometry and characteristics of an ATL L7-4 US probe, used for the experimental investigations described further.

2.2 Experimental measurements

For experimental investigations we used measurement setup described in our previous works on reflection-mode AOI using focused US.^{3,18} It consisted of 532 nm, 6,5 W CW laser (Coherent Verdi 6) and acousto-optic modulator (Gooch Housego, R23080-3-LTD) for emitting 1 μs light pulses. The light was transmitted to the investigated samples using a 200 μm multimode fiber, and then detected using a circular fiber bundle with a

diameter of 4 mm, projecting the optical interference patterns on a sensor of a CCD camera (Allied Vision Stingray F-125B).

The transmitting and receiving fiber facets were positioned 35 mm away from each other, on both sides of an US linear array (elevation direction, centrally). The US transducer was 128. element ATL L7-4 probe. We used detection scheme based on speckle contrast difference measurements, described in our previous studies.^{3,18} We captured pairs of subsequent camera frames, first exposed to 50 laser pulses, and the subsequent one, for which identical number of laser pulses were accompanied by focused or plane wave US pulses, synchronized in such a way, that the illumination occurred when the acoustic wave reached its focus or the desired imaging depth.

The measurements were conducted using cuboid phantoms casted from PVCP with addition of $3,5 \frac{mg}{ml}$ of titanium dioxide, with dimensions of $70 \times 48 \times 35 \text{ mm}^3$. Two phantoms were used: one homogeneous, and one with a cylindrical, optically absorbing inclusion (casted from the same material with addition of black ink) with diameter 3 mm, located centrally, 5 mm below the surface, oriented along the longest edge. The optical and acoustic properties of the phantoms were designed to be within tissue-like value range, with the optical scattering coefficient $\mu_s = 45 \text{ cm}^{-1}$, optical absorption coefficient μ_a negligible for PVCP without ink and equal to approximately 17 cm^{-1} for inclusion, and speed of sound equal $1700 \frac{m}{s}$.

3. RESULTS

The results of the numerical simulations on acoustic pressure field distributions are presented in Figures 1 and 2. Figure 1 presents the examples of results determined for focused US pulses and two focusing depths: 3 mm and 10 mm. Figure 2 presents analogous outcomes of simulations performed for plane wave US pulses and the same imaging depths. The determined distributions were next masked to mimic the assumed, ideal pressure field concentrations only within the desired imaging volumes. The results are presented directly below the corresponding plots. All the components outside the masked regions constitute the residual acoustic pressure field.

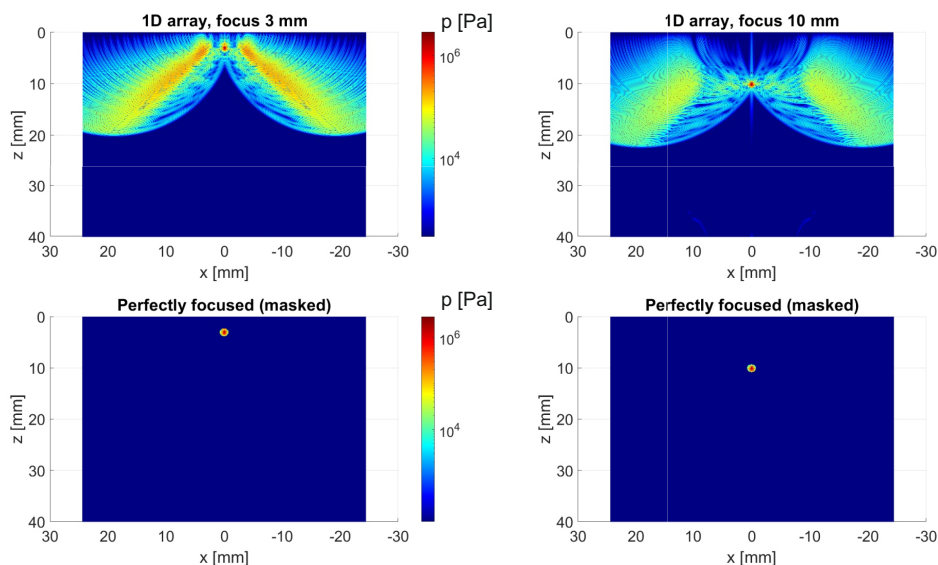


Figure 1. Results of the numerical simulations of acoustic pressure field distributions in axial-lateral planes (cross sections). Top row: ultrasound pulse focused at 3 mm (left) and 10 mm (right). Below are the cross-sections of pressure maps obtained by masking the above distributions with spherical mask located at the desired focal point, in order to simulate the ideal case, without any residual pressure field components.

Figure 3 presents the speckle contrast difference (SCD) values determined for the homogeneous phantom using focused and plane wave US pulses. Value obtained for every single imaging point was obtained by averaging over

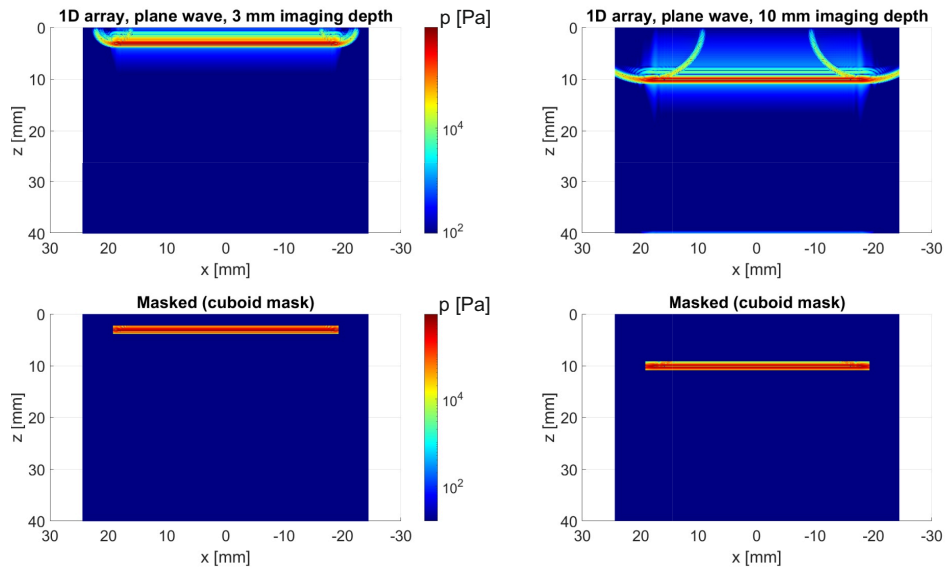


Figure 2. Results of the numerical simulations of acoustic pressure field distributions in axial-lateral planes (cross sections). Top row: plane wave ultrasound pulse propagating at distances 3 mm (left) and 10 mm (right) from the probe. Below are the cross-sections of pressure maps obtained by masking the above distributions with cuboid masks located at the desired imaging depths, in order to simulate the ideal case, without any residual pressure field components.

20 subsequent frame pairs and all 128. transducer elements active. Significant differences between the shape of the obtained curves is clearly visible, particularly in terms of the distinctiveness of the observed local minimum.

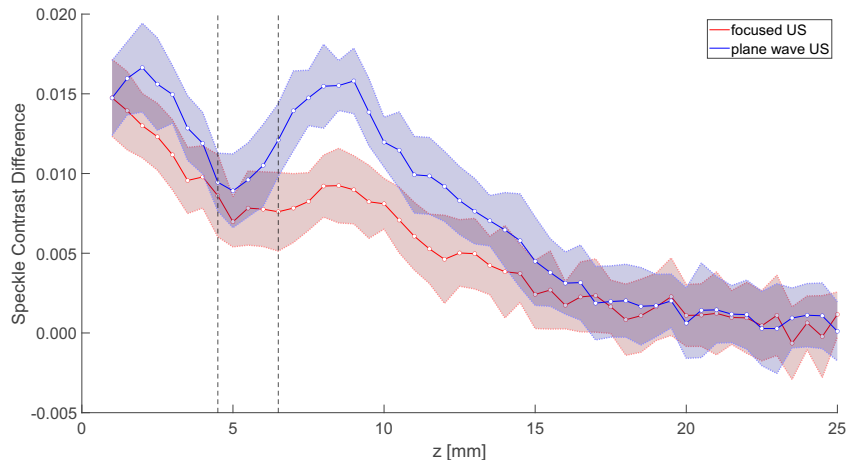


Figure 3. Speckle contrast difference values determined using plane wave and focused US pulses for light modulation along the axial direction, centrally below the probe. The black dashed lines indicate the location of the optically absorbing inclusion inside the imaged phantom.

Figure 4 presents the SCD distributions obtained for the phantom with the inclusion using plane wave pulses. The 2-D scanning was performed by using 32 active US transducer elements at a time and shifting the apodization pattern by 8 elements each step. Different viewing angles and cross-section through the central plane of the determined distribution are introduced.

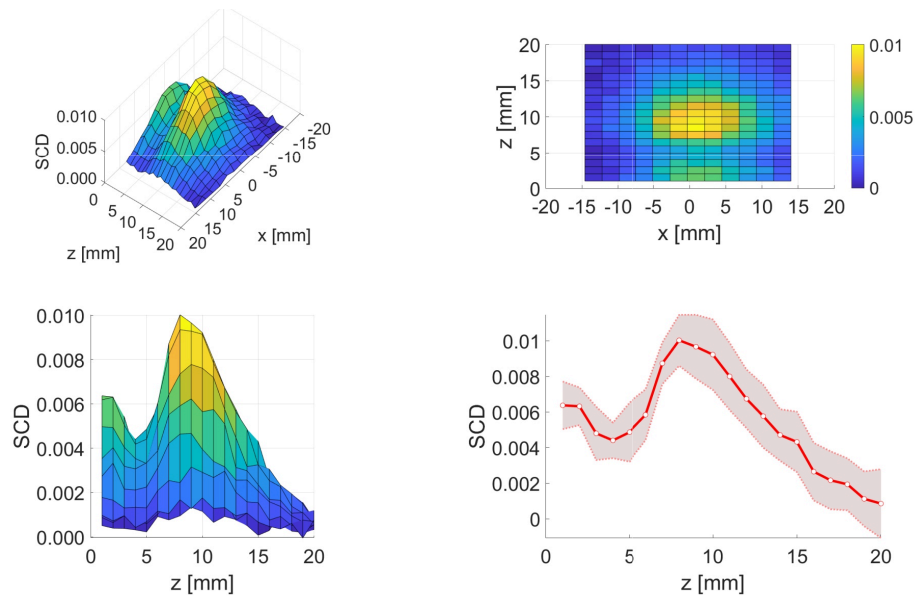


Figure 4. Speckle contrast difference (SCD) distributions determined using plane wave US pulses for phantom with an optically absorbing inclusion of diameter 3 mm, located 5 mm below the surface, and oriented along the US transducer aperture. The 2-D distributions were obtained by using an aperture of 32. active transducer elements, and shifting it with the step of 8. elements.

4. DISCUSSION

Comparison of the acoustic pressure field distributions determined with the numerical simulations (Figures 1 and 2, top rows) to their masked counterparts, mimicking the idealized acoustic characteristics (bottom rows) clearly illustrate the presence of residual pressure field components. The amplitude of those components is lower than in the focal (imaging) region, however they also occupy much greater volume – especially in the case of focused US pulses. Thus, it might be expected that their contribution to the AOI signal will not be negligible.

Forming a single US focus using a 1-D linear array requires applying delays between excitation of subsequent transducer elements in such a manner, that the constructive interference will occur at the desired point. All the elements have identical radiation characteristics, and the resulting pressure amplitude field has complex pattern with a distinct global maximum. Due to the applied delays the residual acoustic components will precede (depth-wise) the US focus. This is not the case for (non tilted) plane wave US pulses, where all the transducer elements are excited at the same time.

The influence of the residual acoustic pressure field components might explain differences in the determined SCD plots, presented in Figure 3. In the case of plane wave AOI the minimum on the plot, corresponding to the location of the optically absorbing inclusion, is much more distinct and clear. This is also due to the fact, that the absorbing inclusion was oriented along the US transducer array, and thus the limited lateral resolution (due to the extent of the imaging region in the plane wave case) was not an issue.

We also demonstrated that 2-D AOI using plane wave US pulses is possible under all the adopted assumptions and with the developed setup. This was achieved by limiting the transducer aperture, and shifting it along the US array in the subsequent imaging steps. In such a way the cross-section scan presented in Figure 4 was obtained. The resulting reconstruction of the light fluence rate is characterized with a single global maximum and a distinct local minimum, corresponding to the location of the optically absorbing inclusion inside the phantom.

ACKNOWLEDGMENTS

Grant 15228 of NWO Division Applied and Engineering Sciences and the Dutch Cancer Society.

REFERENCES

- [1] Leutz, W. and Maret, G., “Ultrasonic modulation of multiply scattered light,” *Physica B: Condensed Matter* **204**, 14–19 (Jan. 1995).
- [2] Wang, L. V., “Mechanisms of Ultrasonic Modulation of Multiply Scattered Coherent Light: An Analytic Model,” *Physical Review Letters* **87**, 043903 (July 2001).
- [3] Nowak, L. J. and Steenbergen, W., “Reflection-mode acousto-optic imaging using a one-dimensional ultrasound array with electronically scanned focus,” *Journal of Biomedical Optics* **25**, 096002 (Sept. 2020). Publisher: International Society for Optics and Photonics.
- [4] Elson, D. S., Li Rui, Dunsby Christopher, Eckersley Robert, and Tang Meng-Xing, “Ultrasound-mediated optical tomography: a review of current methods,” *Interface Focus* **1**, 632–648 (Aug. 2011).
- [5] Resink, S. G., Steenbergen, W., and Boccara, A. C., “State-of-the art of acousto-optic sensing and imaging of turbid media,” *Journal of Biomedical Optics* **17**, 040901 (Apr. 2012).
- [6] Gunther, J. and Andersson-Engels, S., “Review of current methods of acousto-optical tomography for biomedical applications,” *Frontiers of Optoelectronics* **10**, 211–238 (Sept. 2017).
- [7] Lev, A., Kotler, Z., and Sfez, B. G., “Ultrasound tagged light imaging in turbid media in a reflectance geometry,” *Optics Letters* **25**, 378–380 (Mar. 2000).
- [8] Lev, A. and Sfez, B. G., “Direct, noninvasive detection of photon density in turbid media,” *Optics Letters* **27**, 473–475 (Apr. 2002).
- [9] Lev, A. and Sfez, B., “In vivo demonstration of the ultrasound-modulated light technique,” *JOSA A* **20**, 2347–2354 (Dec. 2003).
- [10] Hisaka, M. and Sasakura, Y., “Light Scattering Characteristics of Biological Tissues in Coaxial Ultrasound-Modulated Optical Tomography,” *Japanese Journal of Applied Physics* **48**, 067002 (June 2009).
- [11] Kim, C., Song, K. H., Maslov, K. I., and Wang, L. V., “Ultrasound-modulated optical tomography in reflection mode with ring-shaped light illumination,” *Journal of Biomedical Optics* **14**, 024015 (Mar. 2009).
- [12] Hong-Bo, F., Da, X., Ya-Guang, Z., Yi, W., and Qun, C., “Ultrasound-Modulated Optical Tomography in Reflective and Coaxial Configuration,” *Chinese Physics Letters* **20**, 2165–2168 (Dec. 2003).
- [13] Li, J., Ku, G., and Wang, L. V., “Ultrasound-modulated optical tomography of biological tissue by use of contrast of laser speckles,” *Applied Optics* **41**, 6030 (Oct. 2002).
- [14] Lucas, B. G. and Muir, T. G., “The field of a focusing source,” *The Journal of the Acoustical Society of America* **72**, 1289–1296 (Oct. 1982).
- [15] Laudereau, J.-B., Grabar, A. A., Tanter, M., Gennisson, J.-L., and Ramaz, F., “Ultrafast acousto-optic imaging with ultrasonic plane waves,” *Optics Express* **24**, 3774–3789 (Feb. 2016).
- [16] Bocoum, M., Gennisson, J.-L., Laudereau, J.-B., Louchet-Chauvet, A., Tualle, J.-M., and Ramaz, F., “Structured ultrasound-modulated optical tomography,” *Applied Optics* **58**, 1933–1940 (Mar. 2019).
- [17] Bocoum, M., Gennisson, J.-L., Grabar, A. A., Ramaz, F., and Tualle, J.-M., “Reconstruction of bi-dimensional images in Fourier-transform acousto-optic imaging,” *Optics Letters* **45**, 4855–4858 (Sept. 2020). Publisher: Optical Society of America.
- [18] Nowak, L. J. and Steenbergen, W., “Reflection mode acousto-optic imaging using a 1-D ultrasound array,” in [*Photons Plus Ultrasound: Imaging and Sensing 2020*], **11240**, 112402O, International Society for Optics and Photonics (Feb. 2020).